

TABLE I
RESISTANCE VALUES FOR THREE-PORT HYBRIDS USING
TAPERED IMPEDANCE TRANSFORMER SYSTEMS

Power division ratio, K^2	1	2	3
Chebyshev taper	$R_1 = 2.000$ $R_M = 200.000$	6.000 228.750	8.000 252.193
Exponential taper	$R_1 = 12.000$ $R_M = 212.000$	14.000 234.750	16.000 260.193

these figures is limited but the results shown are typical for higher frequencies as well. In Fig. 4 the frequency scale is normalized to the lower cutoff frequency in gigahertz when the maximum reflection coefficient is 0.05. The characteristics for $K^2 > 1$ are very similar to those shown in Fig. 4 with the isolation showing about a 2-3-dB improvement and the VSWR's for ports 2 and 3 being less than 1.09. In Fig. 5, the frequency scale is normalized to $\beta l = \pi$, where the electrical length (l) of the taper is 15 cm. Again, the characteristics for $K^2 > 1$ are similar to those plotted in Fig. 5. The magnitude of the peak VSWR (above cutoff) for port 1 increases as K^2 increases due to the fixed length of l but remains less than 1.2. VSWRs for ports 2 and 3 have peak values less than 1.15 and the isolation shows an improvement of about 2 dB.

CONCLUSION

The work reported here has extended the analysis of the N -port hybrid to include the use of tapered transmission lines. It has also been shown that the required isolation can be provided by a linear distribution of resistances along the length of the taper. A theoretical limit on the VSWR and isolation characteristics has been presented, along with designs that closely approach this limit. Generally, it has been found that the VSWR and isolation characteristics of the unequal power divider/summer are closely similar to those of the equal power divider/summer.

APPENDIX

ANALYSIS OF THE N -PORT HYBRID FOR ARBITRARY POWER DIVISION

When the N -port hybrid is used for uneven power division, the fractional power level in each arm is determined by the relative admittance of each arm. Therefore, in the equivalent circuit, the divider port characteristic admittance is split into separate admittances such that, at the reference plane of the junction, (Fig. 1, U) we find the following.

1) The ratio of the admittance of that branch to the characteristic admittance of the divider port is equal to the fractional power level in that branch; i.e.,

$$\frac{P_2}{P_1} = \frac{Y_{i2}}{Y_{01}} = K_2$$

$$\frac{P_3}{P_1} = \frac{Y_{i3}}{Y_{01}} = K_3 \cdots \frac{P_N}{P_1} = \frac{Y_{iN}}{Y_{01}} = K_N. \quad (8)$$

2) The parallel combination of the input admittance of the branches is equal to the divider port characteristic admittance:

$$Y_{01} = Y_{i2} + Y_{i3} + \cdots + Y_{iN}. \quad (9)$$

Since the sum of the fractional divided powers equals unity when the matched condition (9) exists,

$$\sum_{i=2}^N K_i = 1. \quad (10)$$

Now the analysis of Parad and Moynihan [2] can be adapted to the N -branch case if we consider that the effect on branch 2 of all the other branches: 3, 4, ..., N , combined, has to be equivalent to the effect of the third branch on the second branch for the three-branch hybrid. From this reasoning, it readily follows that the output im-

pedances R_2, R_3, \dots, R_N should be chosen to be

$$R_2 = Z_{01} \sqrt{(K_3 + K_4 + \cdots + K_N) / K_2}$$

$$R_3 = Z_{01} \sqrt{(K_2 + K_4 + K_5 + \cdots + K_N) / K_3}$$

$$\cdots \cdots \cdots \cdots \cdots \cdots \cdots \cdots$$

$$R_N = Z_{01} \sqrt{(K_2 + K_3 + \cdots + K_{N-1}) / K_N} \quad (11)$$

so that the characteristic admittances of the quarter-wave transformers in arms 2, 3, ..., N are

$$Y_{02} = \sqrt{Y_{i2} G_2} = Y_{01} \sqrt{K_2 [K_3 + K_4 + \cdots + K_N]^{1/2}}$$

$$Y_{03} = \sqrt{Y_{i3} G_3} = Y_{01} \sqrt{K_3 [K_2 + K_4 + \cdots + K_N]^{1/2}}$$

$$\cdots \cdots \cdots \cdots \cdots \cdots \cdots \cdots$$

$$Y_{0N} = \sqrt{Y_{iN} G_N} = Y_{01} \sqrt{K_N [K_2 + K_3 + \cdots + K_{N-1}]^{1/2}}. \quad (12)$$

The isolation resistors required are thus

$$R_{i2} = Z_{01} \sqrt{(K_3 + K_4 + \cdots + K_N) / K_2}$$

$$R_{i3} = Z_{01} \sqrt{(K_2 + K_4 + \cdots + K_N) / K_3}$$

$$\cdots \cdots \cdots \cdots \cdots \cdots \cdots \cdots$$

$$R_{iN} = Z_{01} \sqrt{(K_2 + K_3 + \cdots + K_{N-1}) / K_N} \quad (13)$$

for the special case of a three-port hybrid, we have

$$K^2 = K_3 / K_2. \quad (14)$$

R. P. TETARENKO
P. A. GOUD
Dep. Elec. Eng.
Univ. Alberta,
Edmonton, Alta.
Canada

REFERENCES

- [1] E. J. Wilkinson, "An N -way hybrid power divider," *IRE Trans. Microwave Theory Tech.*, vol. MTT-8, Jan. 1960, pp. 116-118.
- [2] L. I. Parad and R. L. Moynihan, "Split-tee power divider," *IEEE Trans. Microwave Theory Tech.*, vol. MTT-13, Jan. 1965, pp. 91-95.
- [3] S. B. Cohn, "A class of broadband three-port TEM-mode hybrids," *IEEE Trans. Microwave Theory Tech.*, vol. MTT-16, Feb. 1968, pp. 110-116.
- [4] H. Y. Yee, F. C. Chang, and N. F. Audeh, "N-way TEM-mode broad-band power dividers," *IEEE Trans. Microwave Theory Tech.*, vol. MTT-18, Oct. 1970, pp. 682-688.
- [5] R. B. Ekinge, "A new method of synthesizing matched broad-band TEM-mode three-ports," *IEEE Trans. Microwave Theory Tech.*, vol. MTT-19, Jan. 1971, pp. 81-88.
- [6] P. C. Goodman, "A wideband stripline matched power divider," *1968 Int. Microwave Symp. Dig.*, pp. 16-20.
- [7] R. E. Collin, *Foundations for Microwave Engineering*. New York: McGraw-Hill, 1964, pp. 237-250.
- [8] R. P. Tetarenko, "Broadband properties of a class of TEM-mode hybrids," M.Sc. thesis, Dep. Elec. Eng., University of Alberta, Edmonton, Alta., Canada, 1970.

A Wide-Band Nearly Constant Susceptance Waveguide Element

Abstract—Experimental results are presented for a movable metal iris which exhibits a nearly frequency-independent susceptance. This characteristic is related to the susceptance of a centered capacitive obstacle in a waveguide modified by an empirical frequency-dependent correction factor.

Work with waveguide cavities for solid-state microwave devices has led to a movable iris characterized by a shunt susceptance that is nearly constant with frequency. The iris is constructed of a thin rectangular metal strip mounted on a low-loss foam plastic block, as shown in Fig. 1. The block has the same dimensions as the interior of the waveguide and is made long enough to prevent the metal strip from becoming skewed with respect to the waveguide walls. The shim is centered on the foam block, so there is no metal-to-metal contact.

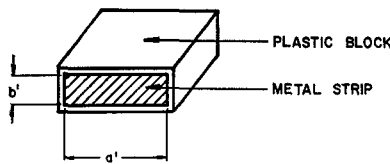


Fig. 1. Noncontacting iris.

The experimental work was done at X band, with internal waveguide dimensions 0.900 by 0.400 in. Six irises were constructed with foam blocks 1-1/2 in long. The metal strip dimensions for each iris are listed in Table I.

The foam block used has a low dielectric constant ($\epsilon \approx 1.05$), and its effect may be neglected. The thin metal shim may be represented by a single shunt susceptance across the waveguide. In general, thin discontinuities parallel to the broad dimension of the waveguide are represented by shunt capacitances, and discontinuities parallel to the narrow dimension are represented by shunt inductances [1]. The shim exhibits discontinuities along both dimensions, but the gap widths are small. For TE_{10} mode excitation an electric field will be excited in the gaps parallel to the broad dimension. The energy stored in the gaps parallel to the narrow dimension of the waveguide will be small since the only significant contribution to the stored energy is due to very high order modes far from cutoff. For this reason the junction can be effectively characterized as a shunt capacitance.

This is verified by the experimental results which are plotted as normalized susceptance as a function of frequency in Fig. 2. The susceptance is capacitive and its magnitude is largely controlled by the b' dimension. Reducing b' lowers the susceptance. The magnitude of the susceptance is approximately the same as that of a centered capacitive obstacle of height b' . The primary effect of the gap parallel to the narrow dimension is to modify the frequency dependence of the capacitance. The resulting susceptance is nearly frequency-independent over the X band.

Several attempts were made to calculate an approximate expression for the iris susceptance. Due to the fact that the iris is discontinuous in both transverse dimensions as well as along the waveguide axis, no simple solution could be obtained. In order to obtain a closed form result suitable for design purposes it was decided to use the calculated susceptance for a capacitive obstacle modified by an empirical correction factor.

The solution is in the form of (1)

$$B_i = \gamma B_c \quad (1)$$

where B_i is the experimental susceptance of the iris, γ is the empirical correction factor, and B_c is the susceptance of a centered capacitive obstacle of height b' . The quantity B_c is obtained from Marcuvitz [2] for the case of the gap much smaller than the narrow dimension of the waveguide. The expression is given in (2),

$$\begin{aligned} \frac{B_c}{Y_0} = \frac{4b}{\lambda_g} & \left\{ \ln \left(\frac{2b}{\pi d} \right) + \frac{1}{6} \left(\frac{\pi d}{2b} \right)^2 \right. \\ & \left. + \frac{1}{2} \left(\frac{b}{\lambda_g} \right)^2 \left[1 - \frac{1}{2} \left(\frac{\pi d}{2b} \right)^2 \right]^4 \right\} \quad (2) \end{aligned}$$

where d is the total gap not filled by the metal obstacle. A correction for the thickness of the obstacle is required so d was taken empirically to be

$$d = b - b' - t \quad (3)$$

where t is the thickness of the metal shim. In this case, $t=0.020$ in, which was not negligible in comparison with the gap dimensions.

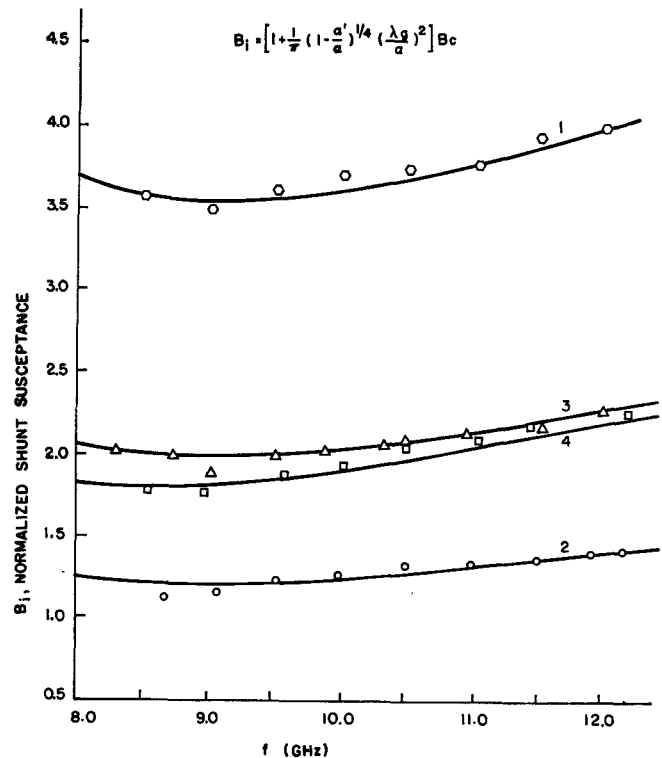


Fig. 2. Comparison between experimental and empirical results.

TABLE I
IRIS DIMENSIONS WITH $t=0.020$ in

Iris	a' (inch)	b' (inch)
1	0.70	0.35
2	0.70	0.25
3	0.70	0.30
4	0.80	0.30
5	0.65	0.30
6	0.55	0.30

For thicker irises the theory given by Marcuvitz [2, p. 251] would be required.

The multiplicative correction factor γ is a dimensionless quantity greater than unity, and is largest at the low end of the frequency band since the susceptance calculated for a capacitive obstacle approaches the measured susceptance as frequency increases. This results in a dependence on λ_g in the correction factor. It is also required that $\gamma \rightarrow 1$ as $a' \rightarrow a$, since the iris becomes a capacitive obstacle in that limit. The form of the correction factor was determined empirically, with the result given in (4)

$$\gamma = 1 + \frac{1}{\pi} \left(1 - \frac{a'}{a} \right)^{1/4} \left(\frac{\lambda_g}{a} \right)^2. \quad (4)$$

The values of B_i obtained by substituting (4) into (1) are plotted as the solid curves in Fig. 2. The results are for the first four irises. The experimental data points are also plotted, and the agreement is seen to be quite good. Irises 5 and 6 are not shown, as the two cases are similar and the experimental data lack sufficient accuracy to distinguish between them. Over the range $0.6 \leq (a'/a) \leq 1$, the accuracy of (1), using (4) is better than ± 8 percent, compared to the experimental results.

The movable iris described here has been shown to provide a nearly-constant capacitive susceptance over the X band. It has been

